Heat Transport Modelling and Adaptive Model Predictive Temperature Control of the Direct Current Plasma Nitriding Process

Nimród D. Kutasi, Emőd Filep, Lajos Kenéz

Department of Electrical Engineering, Faculty of Technical and Human Sciences, Sapientia-Hungarian University of Transylvania, Tg. Mureş, (e-mail: kutasi@ms.sapinetia.ro, efilep@ms.sapientia.ro, l_kenez@ms.sapientia.ro).

Abstract: This paper focuses on exact modelling and model-based predictive temperature control of the direct current plasma nitriding (DCPN) system. The DCPN process is a well-known type of industrial technology. However, the mathematical modelling of this process from a control point of view is not developed. Thus, the aim of this paper is to develop a systematic modelling procedure for heat transport and pressure dynamics. Heat transport modelling was performed taking into account the heat transported by the gas flow, the conducted heat, and the radiated heat. The emissivity of the treated part was estimated and the temperature dependence of the emissivity modelled. Finally, the pressure dynamics was modelled and validated. The model obtained for temperature dynamics is highly nonlinear, mainly due to heat-radiation, and the model contains variable parameters such as the mass of the treated parts. An adaptive model predictive controller (A-MPC) is therefore proposed for accurate temperature control. The performance of the A-MPC is compared with the classical PID controller, proving the benefits of the adaptive model-based control versus the classical model-based control.

Keywords: plasma nitriding, heat transfer, nonlinear model, model predictive control, adaptive control.

1. INTRODUCTION

Plasma nitriding is one of the most developed heat-treatment technologies. It is used when induction heating is inappropriate due to deformation of the treated part, or when special hard thin layers are required on the surface of the part. There are two major plasma nitriding technologies, classical direct current plasma nitriding (DCPN) and active screen plasma nitriding (ASPN). From a control point of view, there are several process variables that need accurate control, the most important being temperature of the treated part, and reactive gas pressure and composition (Rembges et al., 1993; Szatyapal et al., 2013). Control of the aforementioned process variables is similar for both technologies. In this paper the modelling and control of the DCPN process is developed.

There are several papers dealing with the modelling of the plasma nitriding process, but all of these papers present the model of the layer formation during nitriding for certain process conditions. In (Cavaliere et al., 2009), the thermo-chemical diffusional process of nitriding is developed, and in (Guiberteau et al., 1997) pulse glow discharge is modelled. The nitriding process is described in detail in (Kenéz et al., 2013; Mittemeijer, 2013). Closed loop control of the layer formation in the (salt bath) nitriding process, and layer thickness measurement is presented in (Ratajski et al., 2009; 2008). From the process control point of view, (Rembges et al., 1993) presents general aspects of nitriding process control.

To overcome the nonlinear nature of the process, (Filetin et al., 2005) proposed an artificial intelligence-based method and (Oltean et al., 2014) proposed an intelligent system-based process control, namely fuzzy logic-based temperature control.

The aim of this paper is to develop a mathematical model of the process from the control point of view, and thus model the heat transfer during nitriding and develop the treated part's temperature and pressure dynamic equations. The model obtained is used in the following to design a model-based process controller.

This paper is organized as follows. In Section 2, the DCPN process is described and the heat transfer is modelled. The mathematical model of the thermal process contains a temperature-dependent parameter, namely the emissivity of the steel, and in this chapter a new emissivity estimation method is developed and validated. In Section 3, a dynamic model of the process is developed, an adaptive model-predictive controller is designed, and the simulation results are presented. Section 4 contains the conclusions, and section 5 presents the modelling example for the laboratory plasma nitriding system.

2. HEAT TRANSPORT MODELLING

Plasma nitriding takes place in a vacuum chamber, with a possible setup presented in Fig. 1. This chamber has a linear gas flow: the gas mixture enters the chamber at the top while the vacuum pump is on the bottom. The wall of the chamber is the anode and the treated part is the cathode in the case of DCPN. The wall of the chamber is cooled with water, and there is a Langmuir probe feedthrough for plasma diagnostic purposes.

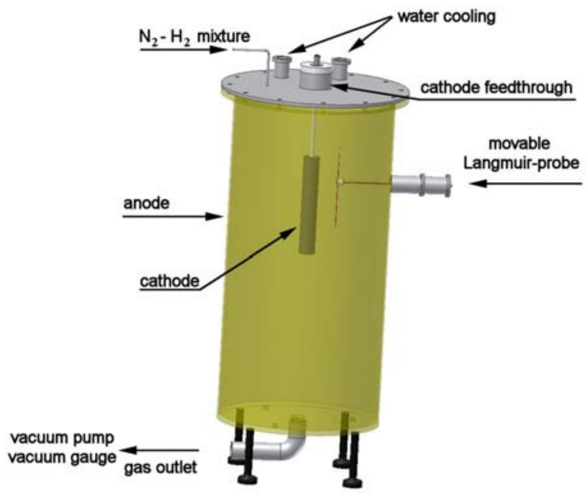

Fig. 1. Linear, non-isotherm plasma reactor used for direct current plasma nitriding.

The schematic principle of the system is presented in Fig. 2.

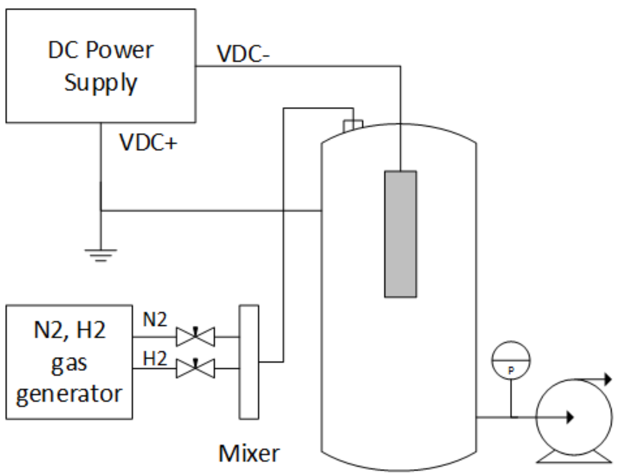

Fig. 2. Plasma nitriding system, consisting of the plasma reactor, DC power supply, gas supply, and vacuum pump.

The plasma reactor is supplied with a high voltage, controlled DC power supply and an N_2-H_2 gas generator. The generator controls the N_2 and H_2 gas flow and the necessary gas mixture is obtained using a mixer. The working pressure in the chamber is given by the inlet gas flow and the pumping speed of the vacuum pump.

In the setup presented the cathode is the part treated, and thus heating this part to the required temperature (usually 810K-873K) and the glow discharge is controlled by the DC power supply. The heat transfer from this part has three mechanisms: Continuous gas flow through the reactor transfers a certain amount of heat from the part to the air through the vacuum pump. The second heat transfer mechanism is heat conduction in the radial direction from the part to the cooled chamber wall. The third and most important heat transfer is through radiation. In the following section the mathematical model of the heat transfer is developed.

2.1 Heat transport by gas flow

To determine the heat power transported by the gas, it is necessary to know the absolute amount of gas. The amount of gas can be calculated using the ideal gas law (1), written to either the inlet gas flow or the outlet gas flow. In this case the outlet gas flow is used due to the fact that the outlet gas pressure is measured.

$$pV = \nu RT \quad \Rightarrow \quad \nu = \frac{pV}{RT} \tag{1}$$

In (1) p is the pressure of the outlet gas (Pa), V is the gas volume (m3), ν is the amount of gas (kmol), R is the ideal gas constant (8310 J/kmolK), and T is the temperature of the outlet gas (K). Taking the time derivative of (1), the mass flow of the gas is obtained (kmol/s).

$$\frac{d\nu}{dt} = \frac{p}{RT}\frac{dV}{dt} \tag{2}$$

The heat power transported by the gas flow is given by (3),

$$P = \frac{d\nu}{dt} C_p \Delta T \tag{3}$$

where P is the power (W), C_p is the heat capacity of the gas (for diatomic gas it is *7R/2*) and ΔT is the temperature rise of the gas. Equation (3) will be used in the power equilibrium equation and in the dynamical model of the system.

2.2 Heat transport by conduction

The thermal conductivity of a gas depends on the nature of the gas and its temperature. The conductivity of a gas mixture is not exactly equal to the weighted average of the component's conductivity. However, in the following model it is considered as the average due to the lack of this data. The typical thermal conductivity of the N_2, H_2 and the calculated mixture's conductivity for different temperatures is presented in Table 1 (Hermann, 1986). The heat flow in the cylindrical chamber in the radial direction is given by the Fourier's first law,

$$P = -\lambda 2\pi rh \frac{dT}{dr} \tag{4}$$

where, λ is the average thermal conductivity, r is the distance measured in the radial direction from the centre of the chamber, h is the high of the cathode, and *dT/dr* is the radial temperature gradient.

Table 1. Thermal conductivity values λ (W/mK).

Temperature (K)	H_2	N_2	$25\%N_2+75\%H_2$
273	0.1593	0.0243	0.1256
373	0.1999	0.0305	0.1576
473	0.2352	0.0362	0.1854
573	0.2666	0.0410	0.2102
673	0.2951	0.0455	0.2306
773	0.3214	0.0497	0.2534
873	0.3458	0.0535	0.2727

From (4), separating the variables,

$$dT = -\frac{P}{\lambda \cdot 2\pi \cdot h}\frac{dr}{r} \tag{5}$$

and defining the limits of the integration as: at the cathode $R_1 \to T_1$, at the anode $R_2 \to T_2$, and in general $r \to T$, from (5) results in:

$$\int_{T_1}^{T} dT = -\frac{P}{\lambda 2\pi h}\int_{R_1}^{r}\frac{dr}{r} \quad \Rightarrow \quad T - T_1 = -\frac{P}{\lambda 2\pi h}\ln\frac{r}{R_1} \tag{6}$$

From (6), the conducted heat power results in:

$$P = \frac{\lambda 2\pi h}{\ln\frac{R_2}{R_1}}\left(T_1 - T_2\right) \tag{7}$$

Equation (7) will be used in the power equilibrium equation, and in the dynamical model of the system.

From (7) and the definitions used in (5), it is possible to determine the radial temperature distribution. From (7), the temperature at distance r from the centre is:

$$T = T_1 - \frac{P}{\lambda 2\pi h}\ln\frac{r}{R_1} \quad where \quad r \in \left[R_1, R_2\right]. \tag{8}$$

The average temperature in the radial direction according to the definition is:

$$\langle T \rangle = \frac{1}{R_2 - R_1}\int_{R_1}^{R_2} T(r)dr \tag{9}$$

2.3 Heat transport by radiation

Heat transfer by radiation is quantitatively the most important power loss in the system. The radiated power is described by:

$$P = \sigma S\left(e_1 T_1^4 - e_2 T_2^4\right), \tag{10}$$

where e_1 is the emissivity of the part and e_2 is the emissivity of the chamber's wall, S is the surface of the cathode (the part), and σ is the Stefan-Boltzmann constant. The emissivity of the part is temperature-dependent variable, so in order to be able to develop an accurate model, it is necessary to obtain the equation for temperature dependence of the emissivity.

2.4 Estimation of emissivity versus temperature

There are two methods described in the literature to determine the emissivity of steel at high temperatures (Paloposki, 2005). The first method, called the SP (SP Swedish National Testing and Research Centre) method is expensive and can only be performed in a laboratory environment, while the second method, called VTT (VTT Technical Research Centre, Finland) is simple but needs an oven to heat up the part and temperature recorder to determine the emissivity. In the following we propose a new, accurate method to estimate the emissivity of steel using the plasma nitriding equipment (Fig.2), without any external measurement devices.

Emissivity estimation has the following principle. Using the plasma nitriding equipment, the investigated part is heated up to 830K using nitriding conditions. When the temperature equilibrium is reached, the gas feed is closed and then the electrical supply is also interrupted. The residual gases are evacuated from the system, and thus a sufficiently low pressure is obtained. In these conditions the cooling speed of the part (cathode) is almost equal to the radiated energy (around 98%), there is a small amount of heat transfer by conduction through the cathode holder, and the chamber wall's radiation can also be considered (all together this is less than 2%, see chapter 5). Recording the cooling curve, the emissivity of the part can be estimated. In the first estimation, only the radiation is considered, and thus the energy balance for the part with a mass of m (kg) is:

$$mc\frac{dT}{dt} = e_1 \sigma S T^4, \tag{11}$$

thus the emissivity is:

$$e_1 = \frac{mc\frac{dT}{dt}}{\sigma S T^4}. \tag{12}$$

In the second approach, the heat conduction of the cathode holder (rod with radius R_r, and length l_r) and the chamber's wall radiation is also considered. The heat loss by conduction is given by Fourier's first law (λ_r is the heat conduction of the rod), thus:

$$Q_2 = \frac{\lambda_r \pi R_r^2}{l_r}\left(T_1 - T_2\right), \tag{13}$$

while the radiation of the chamber wall can be expressed as:

$$Qw = e_2 \sigma S T_2^4. \tag{14}$$

From (11),(13),(14) the resulting total energy balance is:

$$e_1 \sigma S T_1^4 = mc\frac{dT}{dt} + e_2 \sigma S T_2^4 - \lambda_r \pi R_r^2\left(T_1 - T_2\right)/l_r, \tag{15}$$

and the emissivity of the treated part for a given temperature is:

$$e_1 = [mc\frac{dT}{dt} + e_2 \sigma S T_2^4 - \frac{\lambda_r \pi R_r^2\left(T_1 - T_2\right)}{l_r}]/(\sigma S T_1^4) \tag{16}$$

Using (16) and the method described above, in the following the emissivity of C45 carbon steel is determined (for the parameters of the system and the experiment see Section 5). The temperature of the chamber's wall is considered constant (T_2) due to the fact that it is cooled with cooling water. In Fig. 3 the recorded cooling curve is presented.

Using (16) and the derivative of the cooling curve (Fig. 4), the resulting emissivity of the part is as in Fig.5. It is important to notice that the emissivity of the part investigated is highly temperature dependent, and the emissivity value has doubled to within the 300K-873K temperature range. The function obtained is nonlinear, and thus in the mathematical system model, the emissivity will be approximated by a third order function:

$$e\_est(T_1) = a_1 T_1^{\,3} + a_2 T_1^{\,2} + a_3 T_1 \; + a_4 \qquad (17)$$

(In eq. (17) $a_1 = 6.09 \cdot 10^{-9}$, $a_2 = -3.43 \cdot 10^{-6}$, $a_3 = 3.67 \cdot 10^{-4}$, $a_4 = 3.55 \cdot 10^{-1}$).

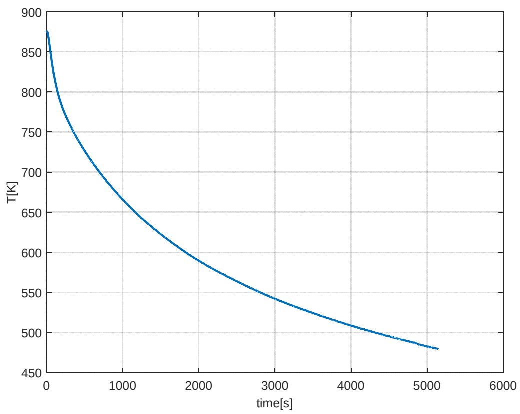

Fig. 3. Cooling curve of the part investigated (starting from 873K).

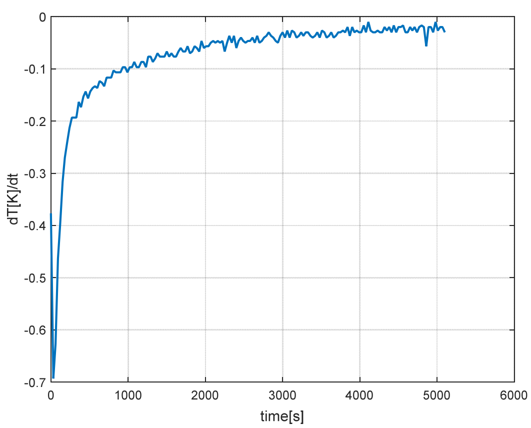

Fig. 4. Derivative of the cooling curve.

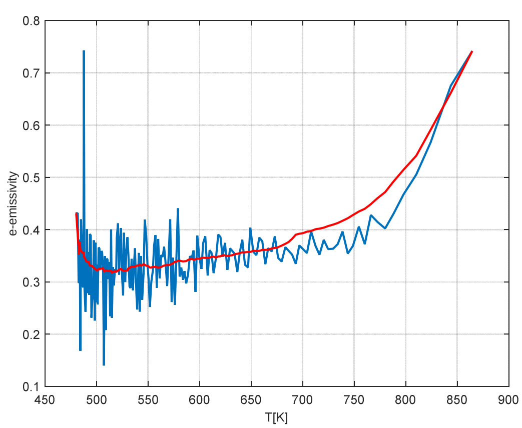

Fig. 5. Estimated emissivity and its filtered values versus temperature.

3. DYNAMIC MODEL OF THE SYSTEM

From the technological and control point of view, there are two process variables that need an exact model: the temperature of the treated part and the pressure of the gas mixture in the chamber. In the following the development of the continuous differential equations describing the temperature and pressure dynamics is presented.

The dynamics of the treated part's temperature results from the heat-power equilibrium equation. The heat quantity necessary to heat up the part with ΔT is:

$$Q = m \cdot c \cdot \Delta T \; , \qquad (18)$$

where m (kg) is the mass off the part and c (J/kgK) is the specific heat. The heating power is given by the derivative of (18), thus:

$$P = \frac{dQ}{dt} = m \cdot c \cdot \frac{dT}{dt} \; . \qquad (19)$$

The effective heating power is equal to the difference between the power introduced and the power loss, thus:

$$\frac{dT}{dt} = \frac{1}{m \cdot c} \cdot \left[P_{in} - P_g - P_c - P_e\right] \qquad (20)$$

where:

- $P_{in} = U \cdot I$ electrical power introduced
- $P_g = \frac{d\nu}{dt} C_p \left(\langle T \rangle - T_2\right)$ heat-power transported by the gas flow (3)
- $P_c = \frac{\lambda 2\pi h}{\ln \frac{R_2}{R_1}} \left(T_1 - T_2\right)$ heat transported by conduction (7)
- $P_e = \sigma S \left(e_1 T_1^{\,4} - e_2 T_e^{\,4}\right)$ radiated heat power (10).

Substituting the expression of each heat-power component in (20), the differential equation of the heating is obtained:

$$\frac{dT_1}{dt} = \frac{1}{m \cdot c} \cdot \begin{bmatrix} U \cdot I - \frac{d\nu}{dt} C_p \left(\langle T \rangle - T_2\right) - \frac{\lambda 2\pi h}{\ln \frac{R_2}{R_1}} \left(T_1 - T_2\right) - \\ - \sigma S \left(e_1 T_1^{\,4} - e_2 T_2^{\,4}\right) \end{bmatrix} \qquad (21)$$

The second control variable is the pressure of the gas mixture in the chamber. The parameters that influence the pressure in the reactor are presented in Fig.6. The inlet gas flow rate (Q_v) is considered after the gas mixer (see Fig.2), while the outlet gas flow rate is determined by the pumping speed of the vacuum pump (S_p).

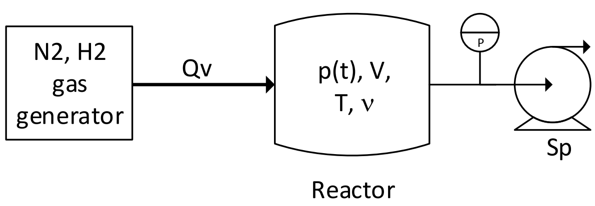

Fig. 6. Gas-feeding of the reactor, the inlet gas flow rate, the parameters that influence the pressure in the chamber, and the pumping speed of the vacuum pump.

The ideal gas law for the reactor, according to (1) is:

There are two variables in (1): the pressure of the gas mixture (p) and the gas amount (ν), thus the time derivative of (1) becomes:

$$\frac{dp}{dt} = \frac{d\nu}{dt}\frac{RT}{V} \tag{22}$$

There are two reasons for the $d\nu$ change in the gas amount: first the $d\nu_1$ gas amount change due to the inlet gas flow rate (Q_v), while the $d\nu_2$ gas amount change is due to the pumping (S_p). Considering (22) for the inlet gas flow:

$$p_1 Q_v = \frac{d\nu_1}{dt} RT \tag{23}$$

and for the outlet gas flow,

$$pS_p = \frac{d\nu_2}{dt} RT \tag{24}$$

The pressure of the inlet gas (p_1) is considered as normal pressure and the temperature of the inlet gas (T) is considered the same as the gas temperature in the reactor due to the reactor's constant cooling.

From (23), (24) and (22) the resulting differential equation of the pressure dynamics in the reactor is:

$$\frac{dp}{dt} = (p_1 Q_v - pS_p)\frac{1}{V} \tag{25}$$

Equations (21) and (25) describe the dynamics of the system. From a control point of view, it is better to consider the applied voltage as an input variable, thus the modelling of the current is also necessary. According to (Kaptzov, 1956), the current in a DC plasma discharge can be expressed by:

$$U = U_n + \frac{k}{p}\cdot(I - I_n)^{1/2} \tag{26}$$

where U is the applied DC voltage, U_n is the minimum voltage level which ensures complete cover with discharge of the cathode, I is the current corresponding to U, I_n the current corresponding to U_n, p is the pressure in the reactor, and k is an empirical, temperature-dependent parameter. From (27) and considering k temperature-dependent ($k'=k/T$) and ($I_n <<$ I), the DC current becomesin:

$$I = \left(\frac{(U - U_n)\cdot\frac{p}{T}}{k'}\right)^2 . \tag{27}$$

Validation of the model for experimental setup is presented in Section 5.

4. CONTROLLER DESIGN

Industrial DCPN equipment is equipped with PID controllers for temperature control. A well-tuned controller can ensure satisfactory control performance for a given temperature setpoint and load parameter. In the hardening workshops, the duty of the reactor varies depending on the required number of treated parts, and thus m – mass is a variable, the emissivity of the part also varies depending on the composition of the steel, and the total surface S of the hardened part changes as well. Consequently, it is hard to design a controller with fixed parameters which can meet the desired control performance. Analyzing this system model, equation (21) is nonlinear and parameter varying due to thermal radiation and the above-presented variations in the process, whereas the second component of the model (25) is linear. In the following section an adaptive model-based predictive controller design is presented in order to overcome the problems of nonlinearity and parameter variation.

Model predictive control has become a reliable solution to control problems where the model of the system is known, there are constraints on the model variables, and an optimal solution is required. In the case of nonlinear models and/or models with parameter uncertainties, there are two typical ways to obtain online linear models: using successive linearization or implementing an online linear model estimator. For details on adaptive MPC and nonlinear MPC, see (Nisha et al., 2015; Bavili et al., 2015; Mathworks, 2015; Medianu et al., 2016).

For the DCPN process the control variables are the temperature of the treated part and the gas mixture pressure, while the inputs are the applied DC voltage and the gas flow rate. Thus, the linear but parameter-varying system's state-space model according to (28) can be considered as a MISO (Multi-Input Single Output) discrete model. The output is considered to be the temperature while the pressure is considered as a disturbance variable due to the fact that the process works at constant pressure determined by the gas generator and vacuum pump (there is no control possibility in the experimental setup: only manual adjustments are possible).

$$\begin{cases} \begin{pmatrix} T(t+1) \\ p(t+1) \end{pmatrix} = A(t)\cdot\begin{pmatrix} T(t) \\ p(t) \end{pmatrix} + B(t)\cdot\begin{pmatrix} U(t) \\ q(t) \end{pmatrix} \\ y(t) = C\cdot\begin{pmatrix} T(t) \\ p(t) \end{pmatrix} \end{cases} \tag{28}$$

The actual system matrix ($A(t)$) and input matrix ($B(t)$) are estimated using a Kalman filter, where *q(t)* is the inlet gas flow rate. First, an ARX regression model (29) is estimated followed by an ARX-SS model transformation.

$$y(t) + A_1 \cdot y(t-1) + A_2 \cdot y(t-2) + \ldots + A_{na} \cdot y(t-na) = B_0 \cdot u(t) + B_1 \cdot u(t-1) + \ldots + B_{nb} \cdot u(t-nb) + e(t) \quad (29)$$

where *y(t)* is the output, *u(t)* is the input, and *e(t)* is white noise.

The adaptive MPC solves the optimal control problems in a receding horizon manner using the current estimated model for the prediction of future states. The principle of the adaptive MPC of the DCPN process is presented in Fig.7.

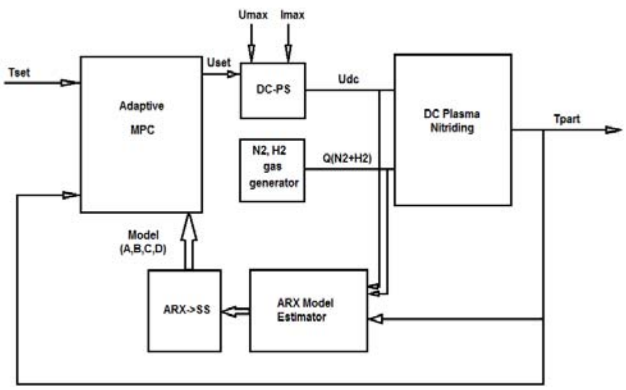

Fig. 7. Block diagram of the proposed adaptive MPC.

The design parameters of the MPC are:

– $N_u = 2$, the control horizon

– $N_y = 10$, the prediction horizon

– Quadratic cost function with weighing $R = 0.1*I$ and $Q = I$ (I-identity matrix).

– Constraints $U_{max} = 1000V$, $U_{min} = 150V$

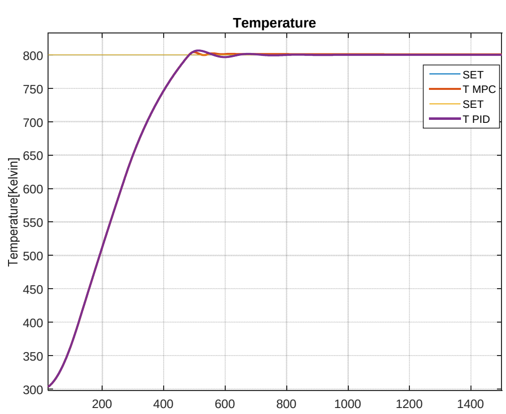

Fig. 8. Temperature control in the case of step change in the setvalue (800K).

The parameters of the system for the simulations are:

– $M = 2.94$kg

– $Qin = 2*10^{-5}$ l/min.

– $T_2 = 300$K.

The simulation results of the adaptive MPC are compared with a well-tuned PID with anty-windup, the simulation results being presented in the following figures.

The adaptive MPC has a shorter settling time and lower overshot, but both controllers perform well, see Fig.8.

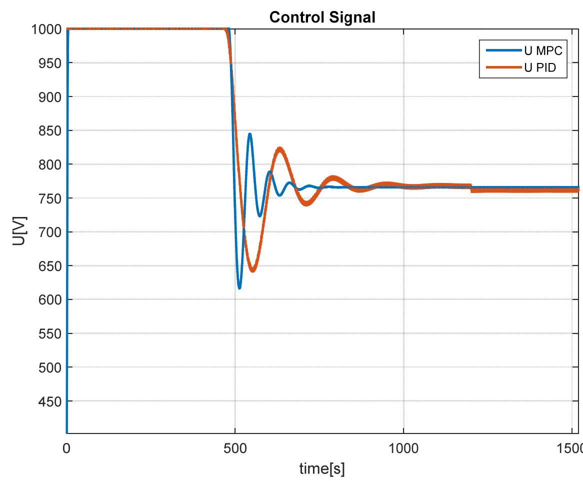

Fig. 9. Control signal (input voltage) in the case of step change in the setvalue.

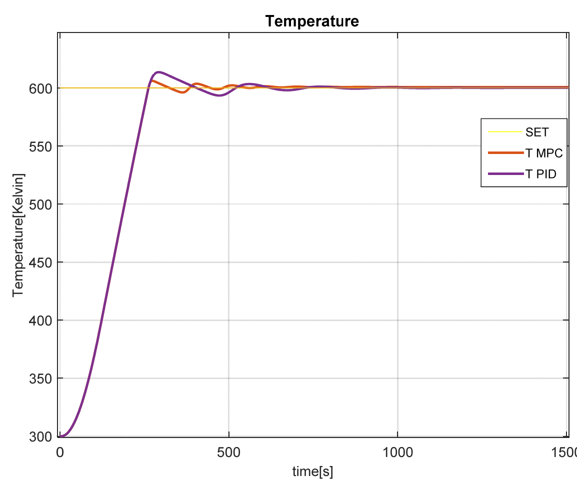

Fig. 10. Temperature control in the case of step change in the setvalue (600K).

According to Fig.10 the benefit of the adaptive MPC is evident.

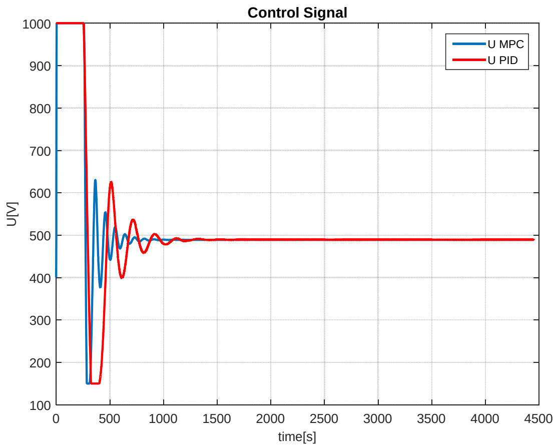

Fig. 11. Control signals in the case of a step change in the setvalue(600K).

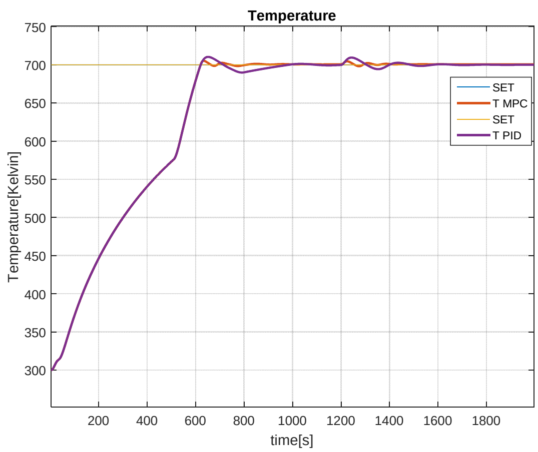

Fig. 12. Temperature control in the case of 700K setvalue and gas-flow perturbation.

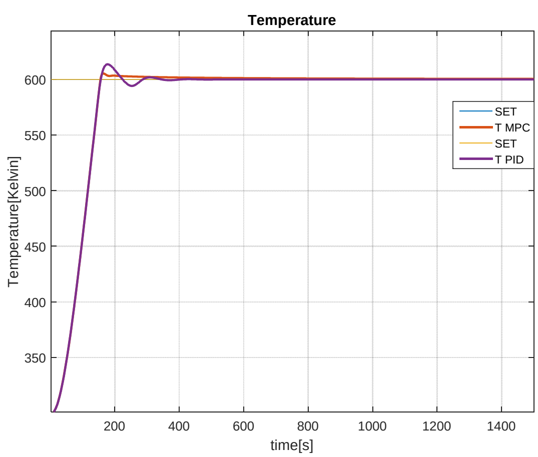

Fig. 13. Temperature control in the case of a change in the mass of the treated part, the total mass having been reduced from m=2.94 kg to m=0.94kg.

The adaptive MPC is "immune" to the parameter change while the PID has a higher overshot.

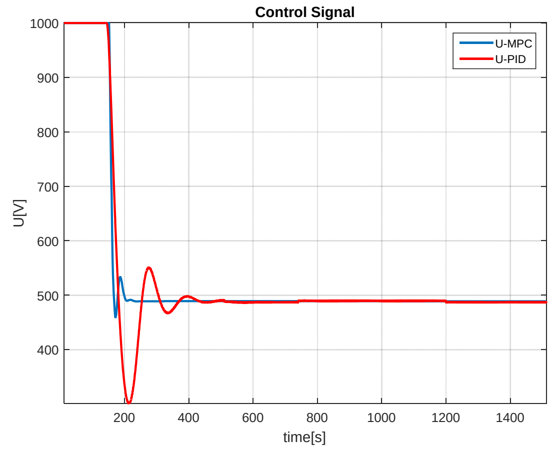

Fig. 14. Control signal in the case of load change.

In Fig.12 at 500s, the inlet gas flow rate has doubled to Q_{in}=2*10^{-5} l/min, at 800s the flow rate became Q_{in}=10^{-5} l/min, and at 1200s Q_{in}=2*10^{-5} l/min. The adaptive MPC has better performance in perturbance rejection.

The simulation results show a clear benefit of the adaptive MPC compared to the PID controller; however, it is difficult to implement due to optimization and estimation algorithms.

5. EXPERIMENTAL SETUP

In this section the experimental setup is presented and the parameters of the system and model validation are described.

Fig. 15. Experimental setup consisting of the plasma reactor, DC power supply, gas generator, vacuum pump, and a PC for process control.

The measurements and calculations were performed using the parameters of the laboratory experimental setup. The working conditions are similar to a real plasma nitriding process.

Parameters of the system:

- Reactor:
  - $Ø$ = 247mm inner diameter (R_2=0.247/2)
  - l = 1000mm, made of aluminum, with double wall (for cooling)
  - Insulated cathode rod made of a $Ø$=12mm steel ($Rr = 6\cdot10^{-3}$ m, $l_r = 0.11m$, $\lambda_r = 16W/mK$)
  - volume V = 50 litres.
  - Wall temperature T_2 = 300K.
  - Emissivity of the wall e_2 = 0.3
- Vacuum pump with pumping capacity $S_p = 4.17\cdot10^{-3}$ m^3/s
- Inlet gas flow rate and composition Qv=150 mL/mn N_2+450 mL/mn H_2, the steady gas pressure in the chamber is p=250 Pa.
- Test part:
  - m=2.94 kg.
  - h=0.204m
  - R_1=0.0485/2 m
  - S=0.03721 m^2
- DC Power supply:
  - Rated power 2.2 kW
  - U_{max}=1200V
  - I_{max}=2000mA
  - Digital control and arc management
- Constants used in the equations:
  - R=8310 J/kmol*K
  - $\sigma=5.67\cdot10^{-8}$ $W/(m^2K^4)$
  - c_{Fe} = 460 J/(kgK)
  - λ_R = 16 W/(mK) – for the rod
  - λ= 0.2 W/(mK) – for the gas mixture
  - C_p=7R/2

To validate the mathematical model, the experimental setup step response and the simulation were examined.

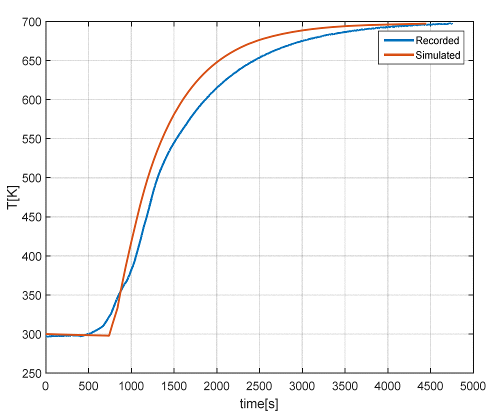

Fig. 16. Temperature development in the case of a 600V step input.

The recorded temperature, voltage and current curves were compared. In the first step, the working pressure of the reactor was set to 250Pa and the power supply was started in arc management mode to clean the workpiece. This behavior can be observed in the first 700s. In the recorded voltage curve, several start/stop (arc discharges) can be observed. Thus, the effective heating of the part takes place from 700s, and therefore the simulation was made in the same manner. The applied voltage was 600V.

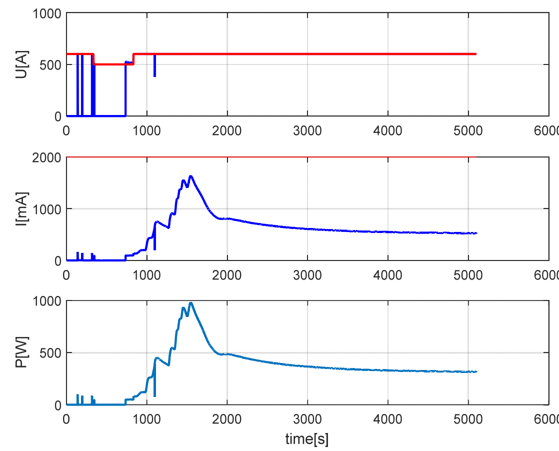

Fig. 17. Recorded voltage, current and power values.

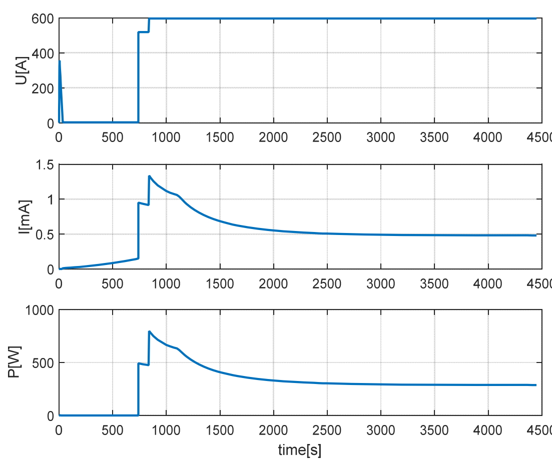

Fig. 18. Simulated voltage, current and power values.

The heat-power values for a given cathode temperature and constant cooling of the reactor was determined, and the effect of the different heat conduction mechanisms was examined. The cathode temperature was considered to be T_1=873K and the wall of the reactor T_2=300K.

According to (3) the transported heat-power depends on the pressure, in this case p=245Pa, the temperature of the outlet gas, T=300K, and the mass flow rate (2):

$$\frac{d\nu}{dt} = \frac{245}{8310\cdot 300}\cdot 4.17\cdot 10^{-3} = 4.09\cdot 10^{-7}\,\text{kmol/s} \qquad (30)$$

Thus the heat loss, calculated for a ΔT=210K temperature rise of the gas around the cathode becomes:

$$P_g = \frac{d\nu}{dt}C_p\Delta T = 4.09\cdot 10^{-7}\,\frac{7}{2}\cdot 8310\cdot 210 = 2.495\,W \qquad (31)$$

The second component of the heat loss is conducted heat, and according to (7):

$$P_c = \frac{\lambda 2\pi h}{\ln \frac{R_2}{R_1}}\left(T_1 - T_2\right) = \frac{0{,}2 \cdot 6{,}28 \cdot 0{,}22}{\ln \frac{247}{48{,}5}}\left(873 - 300\right) = 97\,W \tag{32}$$

The most significant heat loss is due to the radiation (10):

$$\begin{aligned} P_e &= \sigma S\left(e_1 T_1^4 - e_2 T_2^4\right) = \\ &= 5{,}67 \cdot 10^{-8} \cdot 0{,}03721 \cdot \left(0{,}71 \cdot 873^4 - 0{,}35 \cdot 300^4\right) = 855\,W \end{aligned} \tag{33}$$

In conclusion, according to (31), (32), and (33) the radiated heat loss and the conduction loss are around 80-90% and 10-15% respectively , while the heat transported by the gas-flow is less than 1%.

In section 2.4 it is stated that in the conditions presented for estimating the emissivity, the cooling speed of the part (cathode) is almost equal to the radiated energy (around 98%), whereas the heat transfer by conduction through the cathode holder and the chamber walls combined is less than 2%. To prove this assertion, in the following the individual heat loss power conditions from (15) are calculated. The radiated heat loss is 855W according to (33).

The conducted heat loss through the holding rod from (13) is:

$$\begin{aligned} Q_2 &= \frac{\lambda_r \pi R_r^2}{l_r}\left(T_1 - T_2\right) = \frac{16 \cdot \pi \cdot \left(6 \cdot 10^{-3}\right)^2}{0{,}11}\left(T_1 - 300\right) = \\ &= 0{,}01645 \cdot \left(873 - 300\right) = 9.425W \end{aligned} \tag{34}$$

Thus, dividing (34) by (33), the heat loss through conduction in this case is 1.1% from the heat loss due to radiation.

6. CONCLUSIONS

This paper is dedicated to the modelling and control of the direct current plasma nitriding process. The model developed can be used for simulation and controller design, and can be adapted to any configuration of reactor and gas feeding. The model-based control of the process is difficult due to the nonlinearities and parameter variation, and thus an adaptive model-based controller is proposed where the system model is estimated. The resulting controller's performance has been compared to a well known PID controller, for different parameter and setvalue configurations. Further development of the modelling and model-based control is possible for the setup of active screen plasma nitriding.

ACKNOWLEDGMENT

This research is supported by the Institute of Research Programs of the Sapientia University (KPI).

REFERENCES

Bavili, R. E. and Khosrowjerdi, M. J. (2015) Active Fault Tolerant Controller Design using Model Predictive Control, *Journal Of Control Engineering And Applied Informatics*, Vol. 17, No.3, pp.68-76.

Cavaliere, P.,Zavarise G. and Perillo M. (2009) Modeling of the carburizing and nitriding processes, *Computational Materials Science* 46, pp. 26–35.

Filetin T., Žmak I., Lisjak D., Novak D. and Landek D. (2005) The application of artificial intelligence methods in heat treatment. *1st international conference on heat treatment and surface engineering of tools and dies IFHTSE*. Pula, Croatia, pp. 469-476.

Guiberteau, E., Bonhomme, G., Hugon, R. and Henrion. G. (1997) Modelling the pulsed glow discharge of a nitriding reactor, *Surface and Coatings Technology* 97, pp.552–556.

Hermann, E. (1986) Physikalisches Taschenbuch, *Friedr. Vieweg & Sohn: Braunschweig*.

Kaptzov, N.A. (1956) Electronica. Ed.Tehn. Bucuresti, p.293.

Kenez, L., Kutasi, N. Filep, E., Jakab, L.F. and Szocs, I.A.(2013) HeatTreatment of 16MnCr steel in a linear non-isoterm plasma reactor, *Acta Universitatis Sapientiae, Electrical and Mechanical Engineering*, 5, pp. 61-72.

Mathworks (2015) Adaptive MPC - http://www.mathworks.com/help/mpc/ug/adaptive-mpc.html#.

Medianu, S., Lupu C., Lefevre L. and Popescu D. (2016) Solution for Model Adequacy Verification in Indirect Adaptive Control, *Journal Of Control Engineering And Applied Informatics*, Vol. 18, No.1 pp.51-58.

Mittemeijer, E.J. (2013) Fundamentals of Nitriding and Nitrocarburizing. Steel *Heat Treating Fundamentals and Processes, ASM Handbook*; 4(A), pp.619-646.

Nisha, M.G. and Pillai, G. (2015) Nonlinear model predictive control of MIMO system with Least squares support vector machines and Particle swarm optimization*, Journal Of Control Engineering And Applied Informatics*, Vol. 17, No.4, pp.14-22.

Oltean, S.E. and Dulau, M. (2015) Design and Simulation of Fuzzy Logic Based Temperature Control for a Plasma Nitriding Process, *8th International Conference Interdisciplinarity in Engineering, INTER-ENG 2014*, 9-10 October 2014, Tirgu Mures, Romania, Procedia Technology Volume 19, Pages 569–575.

Paloposki, T. and Liedquist, L. (2005) Steel emissivity at high temperatures, VTT Tiedotteita – research note 2299 (http://www.vtt.fi/inf/pdf/tiedotteet/2005/T2299.pdf).

Ratajski, J. and Suszko, T. (2008) Modelling of the nitriding process, *Journal of materials processing technology* 195 22, pp. 212–217.

Ratajski, J., Olik, R., Suszko,T.,Dobrodziej, J., Michalski, J. and Gilewicz A. (2009) Precise formation the phase composition and the thickness of nitrided layers *Journal of Achievements in Materials and Manufacturing Engineering*, 37 (2), pp. 675–689.

Rembges, W. and Oppel, W. (1993) Process control of plasma nitriding and plasma nitrocarburizing in industry, *Surface And Coating Technologies*, Vol 59. Issues 1-3.

Satyapal, M., Khanna, A.S., Alphonsa, J. (2013) Effect of Temperature on the Plasma Nitriding of Duplex Stainless Steels, *International Journal of Engineering and Innovative Technology (IJEIT)*, 2 (11) , pp. 217.